Article

Cell Reports

PLK1 Activation in Late G2 Sets Up Commitment to Mitosis

Graphical Abstract

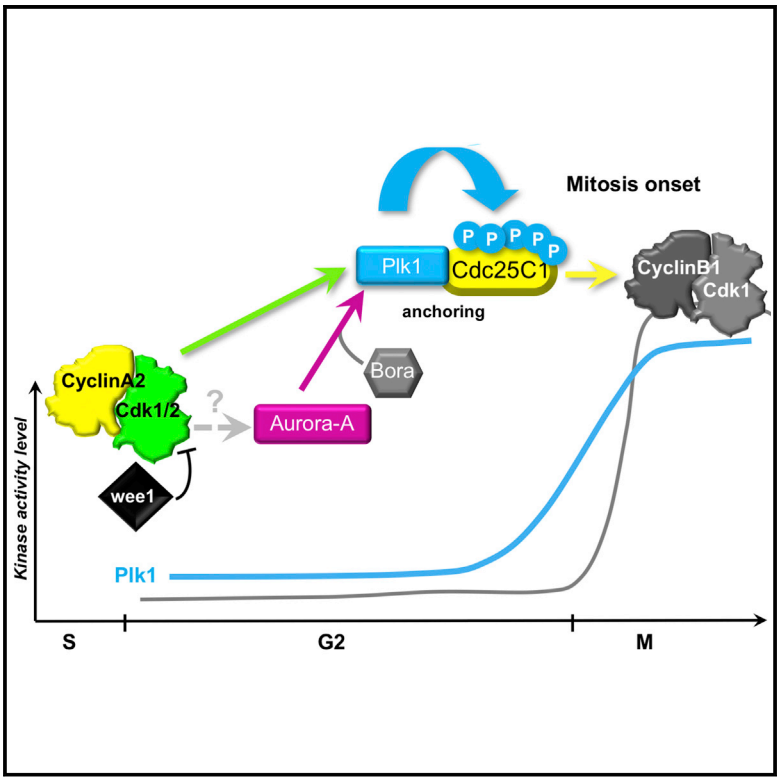

Authors

Lilia Gheghiani, Damarys Loew, Bérangère Lombard, Jörg Mansfeld, Olivier Gavet

Correspondence

olivier.gavet@gustaveroussy.fr

In Brief

Gheghiani et al. find that Plk1 activity is required for commitment to mitosis during normal cell cycles. Sudden Plk1 activation in late G2 is dependent on CyclinA2-Cdk activity levels and triggers Cdc25C1 phosphorylation, promoting mitotic entry.

Highlights

- Plk1 activity is required for commitment to mitosis during normal cell cycles
- Rapid Plk1 activation in late G2 shortly precedes CyclinB1-Cdk1 activation
- CyclinA2-Cdk is an upstream regulator of Plk1 activation
- Plk1-dependent Cdc25C1 phosphorylation promotes mitotic entry

Gheghiani et al., 2017, Cell Reports *19*, 2060–2073
June 6, 2017
http://dx.doi.org/10.1016/j.celrep.2017.05.031

OPEN ACCESS
CellPress

Cell Reports
Article

PLK1 Activation in Late G2 Sets Up Commitment to Mitosis

Lilia Gheghiani,[1,2,3] Damarys Loew,[4] Bérangère Lombard,[4] Jörg Mansfeld,[5] and Olivier Gavet[1,2,3,6,*]
[1]Sorbonne Universités, UPMC University Paris 06, UFR927, 75005 Paris, France
[2]CNRS UMR 8200, 94805 Villejuif, France
[3]Gustave Roussy Cancer Campus, 94805 Villejuif, France
[4]Institut Curie, PSL Research University, LSMP, 75248 Paris, France
[5]Cell Cycle, Biotechnology Center, Technische Universität Dresden, 01307 Dresden, Germany
[6]Lead Contact
*Correspondence: olivier.gavet@gustaveroussy.fr
http://dx.doi.org/10.1016/j.celrep.2017.05.031

SUMMARY

Commitment to mitosis must be tightly coordinated with DNA replication to preserve genome integrity. While we have previously established that the timely activation of CyclinB1-Cdk1 in late G2 triggers mitotic entry, the upstream regulatory mechanisms remain unclear. Here, we report that Polo-like kinase 1 (Plk1) is required for entry into mitosis during an unperturbed cell cycle and is rapidly activated shortly before CyclinB1-Cdk1. We determine that Plk1 associates with the Cdc25C1 phosphatase and induces its phosphorylation before mitotic entry. Plk1-dependent Cdc25C1 phosphosites are sufficient to promote mitotic entry, even when Plk1 activity is inhibited. Furthermore, we find that activation of Plk1 during G2 relies on CyclinA2-Cdk activity levels. Our findings thus elucidate a critical role for Plk1 in CyclinB1-Cdk1 activation and mitotic entry and outline how CyclinA2-Cdk, an S-promoting factor, poises cells for commitment to mitosis.

INTRODUCTION

Commitment to mitosis must be coordinated with the completion of DNA replication to preserve the genetic integrity. Consistently, cells that are induced to enter prematurely into mitosis frequently do not properly divide (Furuno et al., 1999; Karlsson et al., 1999). We previously reported that CyclinB1-Cdk1, the master mitotic driver, is not progressively activated until a specific threshold for mitotic entry but is instead rapidly activated in late G2 triggering prophase onset (Gavet and Pines, 2010a, 2010b). The sudden activation of CyclinB1-Cdk1 indicates that the equilibrium between its upstream phosphatase activators, Cdc25A, B, and C, and inhibitory kinases, Wee1 and Myt1, must be tightly balanced at this time point by still poorly understood mechanisms.

Polo-like kinase 1 (Plk1) has been reported to phosphorylate, at least in vitro, Cdc25B, Cdc25C, Wee1, and Myt1 (Lobjois et al., 2011; Nakajima et al., 2003; Roshak et al., 2000; Watanabe et al., 2005), suggesting that it may be required for CyclinB1-Cdk1 activation. Whereas Plk1 promotes G2 checkpoint recovery, whether its activity is required for entry into mitosis during unperturbed cell cycles remains controversial (van Vugt et al., 2004). Indeed, experiments in which Plk1 was disturbed have generated contradictory results with either a marked G2 arrest (Lane and Nigg, 1996) or a limited G2 delay followed by a mitotic block (Liu et al., 2006; Seki et al., 2008; Sumara et al., 2004), which may emphasize the technical difficulties of effectively inhibiting Plk1. Plk1 depletion in mice is associated with early embryonic lethality and leads either to non-mitotic phenotypes (Lu et al., 2008) or mitotic spindle aberrations with variable penetrance (Wachowicz et al., 2016), which may originate from the progressive dilution of the maternal pool. Similarly, conditional Plk1 depletion in mouse embryonic fibroblasts leads to a limited accumulation of cells into mitosis, possibly linked to the persistence of Plk1 protein during the first cell cycle (Wachowicz et al., 2016).

Here, we report the critical requirement of Plk1 activity for entry into mitosis during normal cell cycles and characterize the upstream and downstream mechanisms by which its activation in late G2 sets up commitment to mitosis.

RESULTS

Plk1 Activity Is Required for Commitment to Mitosis during Normal Cell Cycles

We investigated whether Plk1 activity is required for entry into mitosis during unperturbed cell cycles. Cell cycle progression of asynchronous human immortalized (hTERT-RPE1) and transformed (cervix adenocarcinoma, HeLa) cells were recorded by phase-contrast video-microscopy assays. We used a well-characterized Plk1 inhibitor (BI2536) to reach instant Plk1 inhibition at a set time during recording (Steegmaier et al., 2007). We tested BI2536 compound on asynchronous hTERT-RPE1 cells at increasing concentrations up to 200 nM to reach complete inhibition of Plk1 activity (Burkard et al., 2012). Using BI2536 doses below 20 nM, mitotic progression was delayed, but most cells exited mitosis during recording (data not shown). From 20 to 40 nM, cells were arrested into mitosis for several hours, due

A Asynchronous hTERT-RPE1 cells

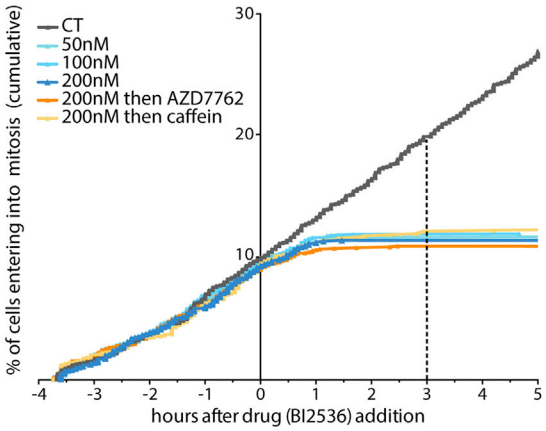

% inhibition at t_{3h} (normalized to CT)	50nM	100nM	200nM
	83	81	90

B Asynchronous HeLa cells

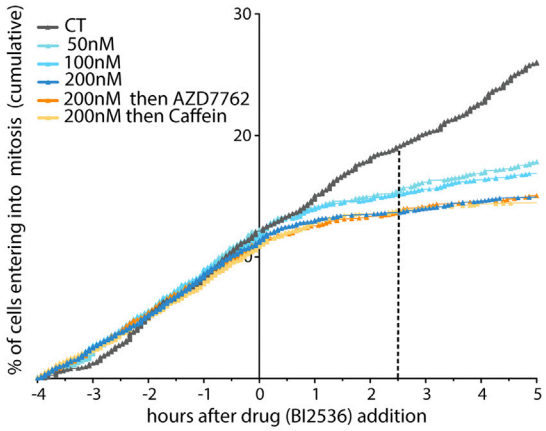

% inhibition at $t_{2.5h}$ (normalized to CT)	50nM	100nM	200nM
	52	57	79

C Asynchronous hTERT-RPE1 cells

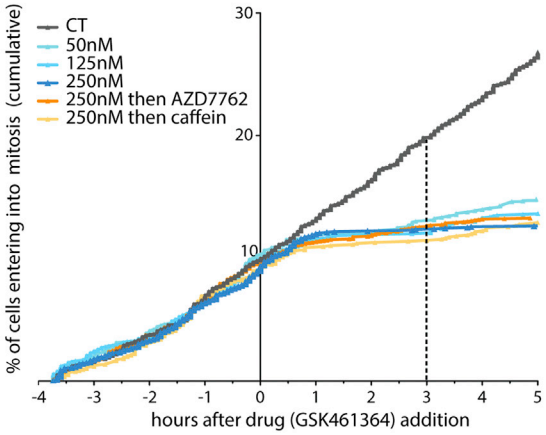

% inhibition at t_{3h} (normalized to CT)	50nM	125nM	250nM
	68	79	76

D Asynchronous HeLa cells

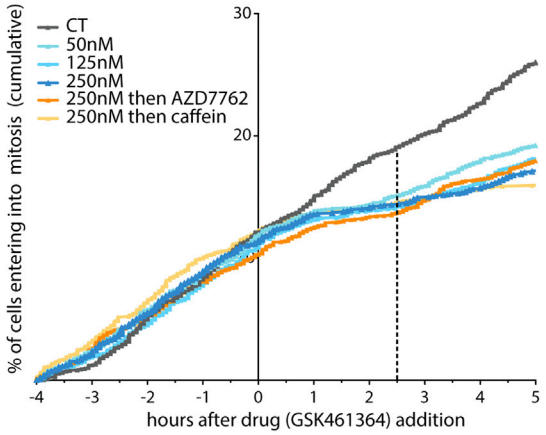

% inhibition at $t_{2.5h}$ (normalized to CT)	50nM	125nM	250nM
	57	70	70

E Asynchronous hTERT-RPE1 PLK1$^{\Delta/\Delta}$ EGFP-Plk1^{WT}

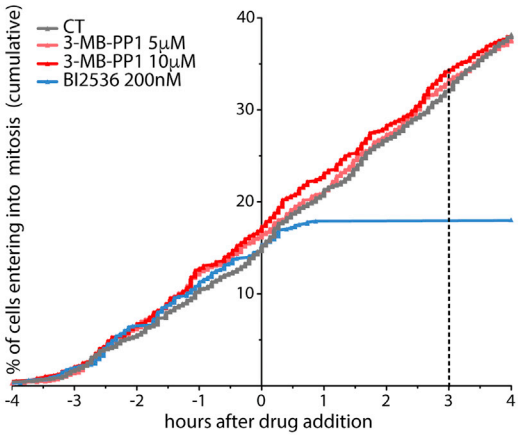

% inhibition at t_{3h} (normalized to CT)	3-MB-PP1: 5μM	10μM	BI2536: 200nM
	0	0	80

F Asynchronous hTERT-RPE1 PLK1$^{\Delta/\Delta}$ EGFP-Plk1^{as}

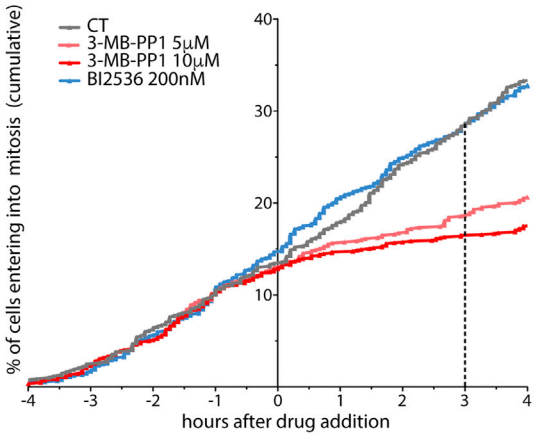

% inhibition at t_{3h} (normalized to CT)	3-MB-PP1: 5μM	10μM	BI2536: 200nM
	62	78	0

(legend on next page)

to spindle assembly checkpoint (SAC) maintenance, with a progressive dose-dependent slowing down of the kinetics of mitotic entry (Figure S1A). From 50 to 200 nM, some cells still entered into mitosis immediately after drug addition, but then mitotic entry became fully inhibited within a 1-hr period (Figures S1A and 1A). Mitotic entry of asynchronous HeLa cells was also strongly inhibited within 1 hr but in a dose-dependent manner from 50 to 200 nM BI2536 (compare Figures 1A and 1B). The differential dose-dependent sensitivity between the two cell lines may rely on the higher Plk1 expression level in HeLa cells (Figure S1B), leading to its incomplete inhibition as investigated thereafter. Previous work established that Plk1 is critical for G2 checkpoint recovery following DNA damage (van Vugt et al., 2004). To rule out that the inhibition of mitotic entry was linked to any activation of DNA damage response (DDR) after drug addition, entry into mitosis was recorded in the presence of BI2536 (200 nM) compound, followed 1 hr later by the addition of caffeine (van Vugt et al., 2004) or a Chk1&Chk2 inhibitor (AZD7762) (Zabludoff et al., 2008), which abrogates G2 checkpoint response. Inhibition of mitotic entry of hTERT-RPE1 or HeLa cells after Plk1 inhibition was not rescued by caffeine or AZD7762 addition (Figures 1A and 1B). Consistently, we did not detect any increase of γ-H2AX or 53BP1 DNA damage foci on hTERT-RPE1 G2 cells (CyclinB1 positive) after BI2536 addition (Figure S1C). Also, the addition of BI2536 compound did not activate p38 MAPK and SAPK/JNK-dependent stress pathways or promote p53 and p21 accumulation (Figure S1D). Inhibition of mitotic entry was further investigated using a different Plk1 inhibitor (GSK461364) that exhibits a 1,000-fold selectivity for Plk1 over Plk2&Plk3 in vitro (Gilmartin et al., 2009). Transition into mitosis of asynchronous hTERT-RPE1 or HeLa cells was strongly inhibited within 1 hr after GSK461364 addition, although this compound exhibited an overall slightly lower efficiency (Figures 1C and 1D). Progression into mitosis could not be rescued by the addition of caffeine or Chk1&Chk2 inhibitor (AZD7762) (Figures 1C and 1D). To confirm the dependency of commitment to mitosis on Plk1 activity during normal cell cycles, we made use of hTERT-RPE1 *PLK1*$^{\Delta/\Delta}$ cells, in which both Plk1 loci have been disrupted, constitutively expressing either EGFP-wild-type Plk1 (EGFP-Plk1^{wt}) or an ATP analog sensitive form (EGFP-Plk1^{as}) (Burkard et al., 2007). Mitotic entry of asynchronous EGFP-Plk1^{wt} -expressing cells was unaffected by the addition of a bulky purine analog (3-MB-PP1) but fully inhibited following BI2536 addition (Figure 1E). Conversely, mitotic entry of EGFP-Plk1^{as}-expressing cells was strongly inhibited following 3-MB-PP1 addition, with a mild dose-dependent effect from 5 to 10 μM but became fully resistant to BI2536 (Figure 1F). This latter observation demonstrates the lack of any side effect of BI2536 compound on the kinetics of mitotic entry. Consistently, using Cdc25C phosphorylation levels as readout of Plk1 activity (see below), we found that Cdc25C phosphorylation in EGFP-Plk1^{as} -expressing cells is insensitive to BI2536 or GSK461364 treatment (Figure S2A). We noted that GSK461364 exhibits a slightly lower efficiency than BI2536 to inhibit Cdc25C phosphorylation in EGFP-Plk1^{wt}-expressing cells (Figure S2A), in good agreement with our time-lapse recordings (Figures 1A–1D). Finally, we analyzed the robustness of the G2 arrest induced by Plk1 inhibition over time. We found that a limited fraction of hTERT-RPE1 *PLK1*$^{\Delta/\Delta}$ EGFP-Plk1^{wt} (Figure S2B) and EGFP-Plk1^{as} (Figure S2C) cells progressively resumed mitotic entry from ~7–8 hr after Plk1 inhibition. Comparison of EGFP levels in cells that resumed mitotic entry versus control conditions showed that Plk1 protein accumulated during the G2 arrest (Figure S2D). To determine whether the resumption of mitotic entry relies on the recovery of Plk1 activity, we combined first Plk1 inhibitor treatment with a second one, 6 or 8 hr later. Importantly, we determined that 3-MB-PP1 or BI2536 can be used at concentrations up to 25 μM or 300 nM, without any side effect on the kinetics of mitotic entry in EGFP-Plk1^{wt} or EGFP-Plk1^{as} cells, respectively (Figure S2D). We found that increasing 3-MB-PP1 or BI2536 concentration decreased the resumption of entry into mitosis in a dose-dependent manner (Figures S2B and S2C), indicating that it relies on Plk1 activity. In addition, pre-incubation assays of 3-MB-PP1 revealed that it is unstable at 37°C, favoring the recovery of Plk1 activity (Figures S2C and S2E).

Altogether, we conclude that Plk1 activity is required to promote commitment to mitosis during normal cell cycles.

Plk1 Activity Rises in Late G2 and Shortly Precedes CyclinB1-Cdk1 Activation

To determine how Plk1 promotes commitment to mitosis, we addressed the regulation of its enzymatic activity in live single-cell assays. We evaluated an improved version of a fluorescence resonance energy transfer (FRET)-based (including a c-Jun substrate sequence) Plk1 phosphorylation sensor highly sensitive to Plk1 depletion or inhibition (Liu et al., 2012), because a first version (including a Myt1 substrate sequence) is phosphorylated to various extents by Plk1 and Mps1, which share closely related target sites, at the time of mitotic entry (Bruinsma et al., 2014). Also, whereas Myt1 and c-Jun-based Plk1 sensors contain identical FHA2 phosphorylation-binding domain (Violin et al., 2003), Myt1-based sensor exhibits slow FRET responses to inhibition of Plk1 as well as phosphatase activities, indicating that it might not be suitable to record rapid variations of Plk1 activity (Figures S3A–S3F). From our data, we hypothesize that its phosphorylation kinetics in the nucleus in G2 (Figure S3A) might reflect a limiting counteracting phosphatase activity (Figure S3C) and

Figure 1. Plk1 Activity Is Required for Commitment to Mitosis during Normal Cell Cycles

(A–F) Entry into mitosis of asynchronous hTERT-RPE1 (A and C), HeLa (B and D), hTERT-RPE1 *PLK1*$^{\Delta/\Delta}$-EGFP-Plk1^{wt} (E), or hTERT-RPE1 *PLK1*$^{\Delta/\Delta}$-EGFP-Plk1^{as} (F) cells were recorded by phase-contrast video-microscopy at one image/4 min in the indicated conditions. Entry into mitosis for each cell was defined at NEBD. (A–F) n > 1,000 cells for each condition; two independent experiments. Graphs represent the percentage of cells that have entered into mitosis over time, normalized to cell density. Tables report the percentage of inhibition of mitotic entry, normalized to control (CT), at 3 (RPE1) or 2.5 (HeLa) hr after drug addition. These times correspond to average G2 phase duration as previously determined using PCNA staining (data not shown). (A–D) Caffeine (5 μM) or Chk1&Chk2 inhibitor (AZD7762 100 nM) were added 1 hr after Plk1 inhibition.

See also Figures S1 and S2.

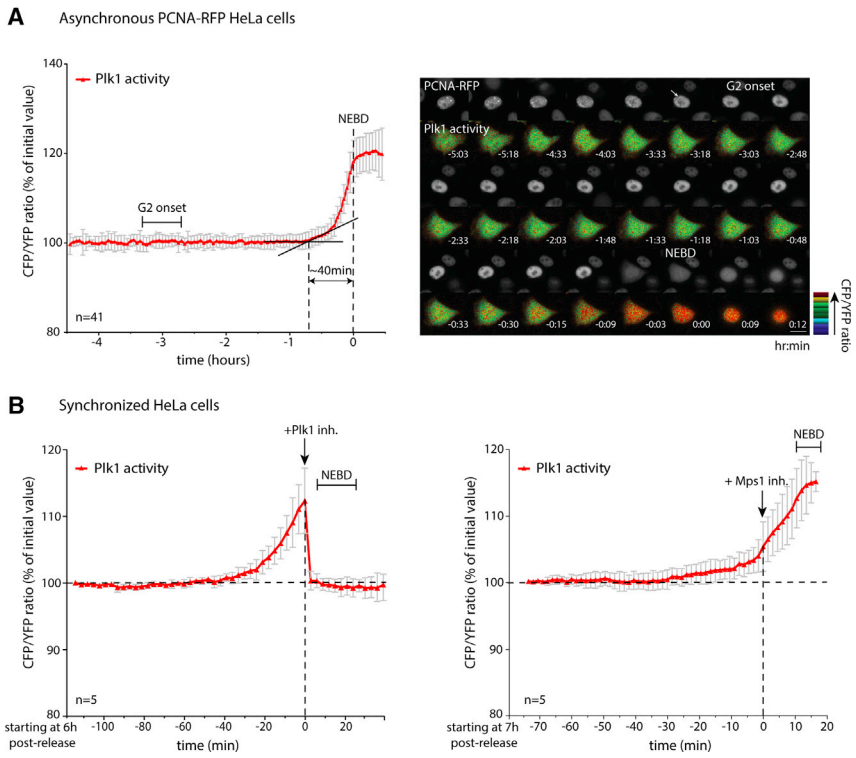

Figure 2. Plk1 Activity Suddenly Rises in Late G2

(A) Asynchronous PCNA-RFP HeLa cell line transiently expressing the (c-Jun based) Plk1 sensor. Recording was performed at one image/3 min. Curves were aligned on NEBD. Data are means ± SD, n = 41 cells; three independent experiments. Right: PCNA staining and IMD representation of CFP/YFP emission ratio changes over time.

(B) Synchronized (single thymidine release regime) HeLa cells expressing the Plk1 sensor were treated with Plk1 (BI2536 200 nM, left) or Mps1 (reversine 5 μM, right) inhibitor at mitosis onset. Curves were aligned on the time of drug addition. Mean quantification curves (±SD) of emission ratio changes are displayed (n = 5; two independent experiments). Bar, 10 μm. See also Figures S3 and S4.

relies on Plk1 protein accumulation exhibiting a minimal kinase activity (Figure S3B).

C-Jun-based Plk1 sensor (hereafter referred to as Plk1 sensor) exhibited a FRET signal increase of around 20% between interphase and mitotic cells, as described in more detail thereafter. Hence, mitotically arrested HeLa cells expressing the Plk1 sensor were treated with either Mps1 (reversine + MG132 to avoid any mitotic exit) or a Plk1 (BI2536) inhibitor. Whereas Plk1 inhibition induced its complete dephosphorylation to interphase level within ~6 min, this sensor was insensitive to the addition of a Mps1 inhibitor (Figure S3D). Similar experiments performed on interphase (G2 phase-enriched) cells did not show any change of Plk1 sensor phosphorylation level (Figure S3E). Interphase Plk1 sensor-expressing cells were also detached from their substratum by trypsin treatment, which showed that the FRET signal was insensitive to cell rounding up as normally taking place at mitotic entry (Figure S3E). Because FRET-based Plk1 sensor records the balance between Plk1 and opposite phosphatase(s) activity, we investigated whether its phosphorylation during mitosis relies on a downregulation of counteracting phosphatase(s). FRET signal was monitored in mitotic versus G2-enriched cells after the addition of a PP2A&PP1 inhibitor (okadaic acid) (Figures S3E and S3F). This treatment led within 5 min to a pronounced increase in sensor phosphorylation in mitotic cells, whereas its phosphorylation level was barely increased in G2 cells. Hence, the increase of Plk1 sensor phosphorylation during mitosis is not due to the inactivation of counteracting phosphatase(s). Altogether, our data indicate that the c-Jun-based Plk1 sensor is ideally suited to investigate the spatiotemporal regulation of Plk1 activity per se.

We carried out analysis of Plk1 activity during the cell cycle in asynchronous proliferating cell nuclear antigen (PCNA)-RFP-expressing HeLa cells. No significant change of Plk1 activity was detectable from G2 onset corresponding to the initiation of Plk1 protein synthesis (Akopyan et al., 2014). Remarkably, a rapid Plk1 activity increase reproducibly occurred in late G2, around 40 min before nuclear envelope break down (NEBD) (Figure 2A). Addition of either a Plk1 or a Mps1 inhibitor shortly before NEBD confirmed that the activation kinetics recorded is strictly dependent on Plk1, but not Mps1, activity (Figure 2B). This activation kinetics was almost identical between nuclear and cytoplasmic compartments on mitotic entry (Figure S4A), although in most cells a basal Plk1 activity was detectable in the nucleus possibly related to its local activation/roles at centromeres in G2 (McKinley and Cheeseman, 2014). Consistent with the sudden Plk1 activity increase observed in late G2, immunostaining assays of CyclinB1 Ser133 phosphorylation, a well-characterized Plk1 phosphorylation site in vivo (Jackman et al., 2003), showed that its phosphorylation does not increase during G2 (as visualized by CyclinB1 accumulation) but is rapidly taking place around mitotic entry (Figure S4B).

We compared the activation kinetics of Plk1 versus CyclinB1-Cdk1 during G2/M transition. HeLa cells co-expressing the Plk1 sensor and CyclinB1-mCherry were used for this purpose as CyclinB1 nuclear translocation in early prophase is concurrent and dependent on CyclinB1-Cdk1 activation (Gavet and Pines, 2010b), making CyclinB1 nuclear translocation a surrogate marker of CyclinB1-Cdk1 activation. Because Plk1 activation kinetics at mitotic entry was similar between asynchronous and synchronized (thymidine-release regime) HeLa cells (Figures 3A and 3B), cells were enriched in G2 and recorded at one image/45 s to get a high temporal resolution. In all cells analyzed, Plk1 activation shortly preceded the nuclear translocation of CyclinB1-Cdk1, with a mean interval between the two processes of 18 ± 4 min (Figure 3B). We addressed the relationship between Plk1 and CyclinB1-Cdk1 activation by performing

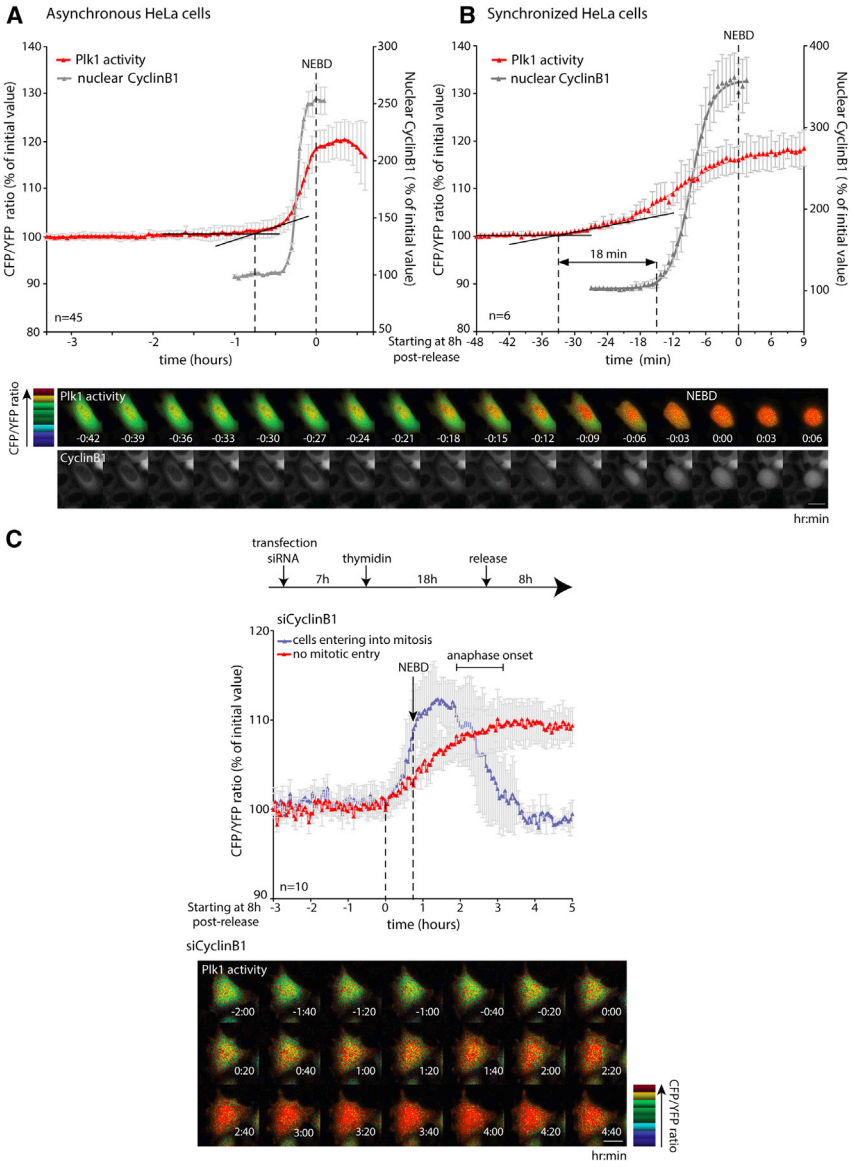

Figure 3. Plk1 Activity Rise Shortly Precedes CyclinB1-Cdk1 Activation

(A) Asynchronous CyclinB1-mCherry HeLa cell line transiently expressing the Plk1 sensor. Recording was performed at one image/3 min. Curves were aligned on NEBD. Data are means ± SD, n = 45; two independent experiments.

(B) Synchronized CyclinB1-mCherry HeLa cell line transiently expressing the Plk1 sensor (one image/45 s). Curves were aligned on NEBD. Data are means ± SD, n = 6; three independent experiments. Bottom: IMD representation of CFP/YFP ratio changes and CyclinB1 nuclear translocation at mitotic entry are displayed (one selected image each 3 min).

(C) CyclinB1-mCherry and Plk1 sensor HeLa stable cell line was recorded at one image/3 min, ~33 hr after RNAi-mediated CyclinB1 depletion. Curves display CFP/YFP emission ratio changes during time in cells that either achieved mitotic entry or did not enter into mitosis. Data are means ± SD, n = 10 per condition; two independent experiments. Curves were aligned on NEBD or on the first time point of CFP/YFP increase, respectively. Bottom: IMD representation of CFP/YFP ratio changes in a cell that did not enter into mitosis.

Bars, 10 μm. See also Figure S4.

CyclinB1 knockdown assays. The use of HeLa cells stably expressing CyclinB1-mCherry to get a direct readout confirmed the overall efficiency of RNAi-mediated CyclinB1 depletion (Figure S4C). Hence, changes of Plk1 activity during time were analyzed in cells that either did not enter mitosis or instead that still achieved mitotic entry, due to incomplete CyclinB1 depletion. In the latter ones, the timing of Plk1 activation (starting ~45 min before NEBD) appeared unaffected, whereas maximum Plk1 activity reached at NEBD was significantly reduced (Figure 3C). More importantly, Plk1 activation was taking place in cells that did not achieve mitotic entry although with a slower kinetics. Hence, our results support that Plk1 activation in late G2 is initiated independently of CyclinB1-Cdk1 activity although feedback mechanisms might be taking place following CyclinB1-Cdk1 activation (Lindqvist et al., 2009).

Finally, we investigated why some transformed HeLa cells continued to achieve mitotic entry in the presence of a high dose of a Plk1 inhibitor (BI2536 200 nM), in contrast to immortalized hTERT-RPE1 cells (Figures 1A and 1B). In all transformed cells that still entered mitosis, a Plk1 activity increase preceded mitotic entry (starting ~50 min before NEBD), although maximum Plk1 activity reached at NEBD was significantly lower (FRET dynamic range <5% versus up to 20% in CT conditions) (Figure S4D). Subsequent increase of Plk1 inhibitor concentration immediately induced Plk1 sensor dephosphorylation, confirming that its phosphorylation preceding mitotic entry was dependent on a remaining Plk1 activity (Figure S4D). Therefore, it supports the conclusion that transformed cells do not achieve mitotic entry by Plk1-independent mechanisms and that a minimal Plk1 activity is sufficient to promote commitment to mitosis.

In summary, we found that Plk1 activity suddenly rises in late G2 and shortly precedes CyclinB1-Cdk1 activation, providing insights into the role of Plk1 in promoting entry into mitosis during normal cell cycles.

CyclinA2-Cdk Is an Upstream Regulator of Plk1 Activation during G2

We investigated the upstream mechanisms leading to Plk1 activation. Consistent with previous findings, sudden Plk1 activation in late G2 is dependent on Aurora-A activity (Figure S4E)

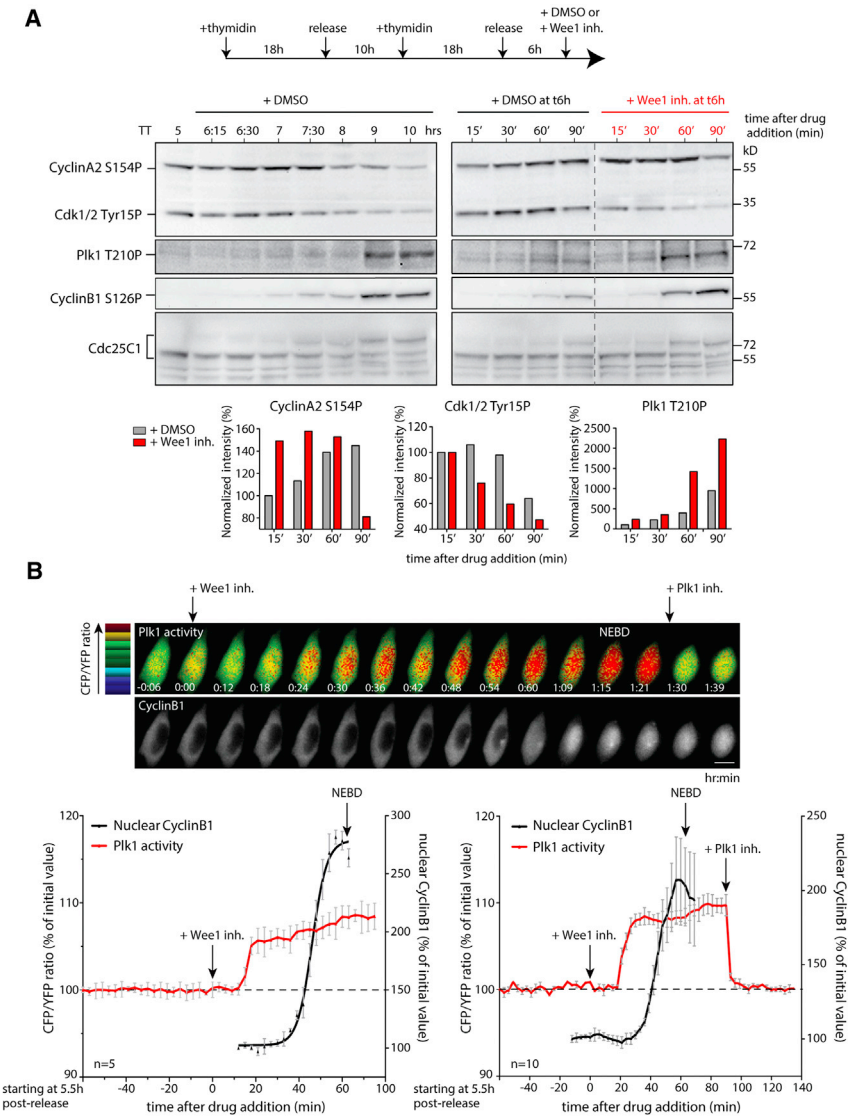

Figure 4. Stimulation of CyclinA2-Cdk Activity in Early G2 Induces a Premature Activation of Plk1

(A) Following a double thymidine (TT) release regime, HeLa cell extracts at reported times were analyzed by immunoblot. Left: phosphorylation profiles during cell-cycle progression. Right: comparison of phosphorylation profiles between CT (DMSO) and Wee1 (MK-1775) inhibitor-treated cells at t_{6h} post-release. Bottom: normalized quantification of corresponding immunoblots. n = 2.

(B) Early G2 synchronized HeLa cells co-expressing the Plk1 sensor and CyclinB1-mCherry were treated by Wee1 inhibitor MK-1775 followed or not by Plk1 inhibition (BI2536) ~90 min later (right). Data are means ± SD. Left: n = 5, right: n = 10; three independent experiments. Top: IMD representation of CFP/YFP ratio changes and CyclinB1 intracellular localization during time in the indicated conditions. Bar, 10 μm. See also Figure S5.

(Macůrek et al., 2008; Seki et al., 2008). Also, Aurora-A and/or Plk1 activation rely on a Cdk activity that remains ill defined (Van Horn et al., 2010; Lorca et al., 2010; Marumoto et al., 2002; Seki et al., 2008). We sought to determine whether CyclinA2-Cdk acts upstream of the Aurora-A → Plk1 pathway. While CyclinA2-Cdk is a limiting factor for mitotic entry, the underlying mechanism is currently unknown (Fung et al., 2007; Gong et al., 2007). CyclinA2-Cdk1&2 complexes exhibit biphasic activation kinetics with a limited activity in S phase and a progressive increase during G2 (Goldstone et al., 2001; Pagano et al., 1992). CyclinA2-Cdk2 is regulated by Wee1-dependent Tyr15 phosphorylation and in contrast to CyclinB1-Cdk1 is a poor substrate of Myt1 kinase (Booher et al., 1997; Coulonval et al., 2003). Also, the contribution of cytoplasmic and membrane-anchored Myt1 in the regulation of mainly nuclear CyclinA2-Cdk1&2 complexes may be limited by their differential intracellular distribution (Figure S5A). Hence, we made use of Wee1 inhibitor MK-1775 (>100-fold selectivity over Myt1) to prematurely raise CyclinA2-Cdk activity in early G2. Addition of MK-1775 on early G2 cells (~6–7 hr post-thymidine release, as determined using a PCNA-RFP marker) induced a premature mitotic entry of the cell population by at least 1 hr (Figure S5B). Interestingly, the kinetics of CyclinB1 nuclear translocation at prophase remained unaffected, whereas mitotic exit was frequently delayed in these conditions (Figure S5C). Immunoblot assays revealed that Wee1 inhibition in early G2 stimulated CyclinA2-Cdk activity within 15–30 min as visualized by a phospho-specific antibody directed against the CyclinA2-S154 autophosphorylation site (Figures 4A and S5D) (Pagliuca et al., 2011). A concurrent decrease in Cdk1/2 Tyr15 phosphorylation was also observed (Figures 4A and S5D). More importantly, compared to normal cell-cycle conditions, Wee1 inhibition caused a premature Plk1 activation by up to 1.5 hr (Figure 4A). Premature CyclinB1-Cdk1 activation ~60 min after Wee1 inhibition, as revealed by the use of a phospho-specific antibody against the S126 auto-phosphorylation site, and Cdc25C hyperphosphorylation were also observed (Figure 4A). To get access to the kinetics of Plk1 activation following Wee1 inhibition, we performed time-lapse single-cell assays. Early G2 cells co-expressing the Plk1 sensor and CyclinB1-mCherry were treated with Wee1 inhibitor MK-1775. This treatment reproducibly induced within 10–20 min a premature activation of Plk1 by around 1.5 hr, consistent with our biochemical results (Figure 4B, left). The extent of maximum Plk1 sensor phosphorylation was significantly lower in these conditions (FRET dynamic range of up to 10% versus ~20%) (Figures 3B and 4B), which might be related to the lower expression level of Plk1 in early G2 (Akopyan et al.,

2014). Remarkably, reminiscent to the normal cell cycle, Plk1 activation still preceded the onset of CyclinB1 nuclear translocation by the same duration (~20 min) (Figure 4B, left). The subsequent addition of BI2536 compound confirmed that the premature phosphorylation of Plk1 sensor in early G2 was dependent on Plk1 activity (Figure 4B, right).

To unravel how CyclinA2-Cdk may trigger Plk1 activation, we investigated whether a molecular interaction between them is taking place during cell cycle progression. To this end, we made use of a CyclinA2-mVenus/$^{+}$ (mRuby-PCNA/$^{+}$ double knockin) hTERT-RPE1 cell line. Endogenous CyclinA2 (-mVenus) was exclusively nuclear in S phase but slowly accumulated in the cytoplasm during G2. Its intracellular distribution between both compartments was not significantly affected following Wee1 inhibition (our unpublished data). Immunoprecipitation of mVenus-tagged CyclinA2 from synchronized RPE-1 cells revealed that Plk1 progressively interacted with CyclinA2 during G2 progression (mitotic peak ~10 hr post-release), related to the increase of CyclinA2-Cdk activity (Figure 5A, right). Conversely, this interaction appeared unrelated to Plk1 and CyclinA2 protein expression levels (Figure 5A, left). Addition of the Wee1 inhibitor induced a rapid decrease of CyclinA2-associated Cdk1/2 Tyr15 phosphorylation and significantly promoted endogenous CyclinA2-Plk1 interaction (Figure 5A, right).

Altogether, these findings strongly suggest that Plk1 activation during G2 is dependent on CyclinA2-Cdk activity levels, providing an outline on how the latter kinase contributes to the control of mitotic entry.

Because Plk1 activation preceded a premature mitotic entry following Wee1 inhibition (Figure 4B), we asked whether its activity was still required to promote entry into mitosis in these conditions. Early G2 cells were first treated by the Wee1 inhibitor followed 40 min later by the addition of Plk1 inhibitor BI2536. Plk1 inhibition induced within a few minutes a pronounced decrease in mitotic entry (Figure 5B), supporting that its activity is required in a premature transition into mitosis. A complementary experiment in which Plk1 activity was inhibited before Wee1 inhibition provided the same results and supported this interpretation (Figure 5C). We sought to induce a premature mitotic entry by targeting both Wee1 and Myt1 inhibitory kinases of CyclinB1-Cdk1 (Wee1&Myt1 inhibitor PD166285) (Gaffré et al., 2011). In these conditions, entry into mitosis was strongly promoted but remarkably remained unaffected following Plk1 inhibition (Figure 5B). Consistently, immunoblots showed that the premature activation of CyclinB1-Cdk1 is dependent on Plk1 activity following Wee1, but not Wee1&Myt1, inhibition (Figure 5D). Together, it supports the conclusion that, in normal cell cycles as well as during unscheduled mitotic entry following CyclinA2-Cdk stimulation, Plk1 is activated shortly before CyclinB1-Cdk1 and its activity is required for commitment to mitosis.

Plk1-Dependent Cdc25C1 Phosphorylation in Late G2 Promotes Entry into Mitosis

We addressed the mechanisms by which Plk1 promotes entry into mitosis. Cdc25A, B, and C phosphatases, although partially redundant, are involved in CyclinB1-Cdk1 activation (Lee et al., 2009; Lindqvist et al., 2009). Plk1 can phosphorylate both Cdc25B and Cdc25C in vitro, but it remains poorly characterized which Cdc25 phosphatase(s) are substrates of Plk1 during the transition into mitosis (Lobjois et al., 2011; Roshak et al., 2000). To tackle this point, we analyzed Cdc25A, B, and C phosphorylation states by two-dimensional gel electrophoresis following or not Plk1 inhibition on mitotically arrested HeLa cells. We found that Cdc25C, but not Cdc25A or Cdc25B, displayed phosphorylated forms ("P") that exhibit an isoelectric point shift following Plk1 inhibition (Figure 6A). Lower exposure (inserts) indicated that it corresponds to up to four highly phosphorylated forms probably phosphorylated on combinations of both Plk1 and Cdk1 sites, because these forms persist after Plk1 inhibition. Remarkably, of the two major Cdc25C1 and Cdc25C5 isoforms expressed, as determined by RT-PCR (data not shown), only Cdc25C1 was phosphorylated in a Plk1-dependent manner (Figure 6A) (Albert et al., 2011). Consistently, endogenous Plk1 co-immunoprecipitated with 3xFLAG-tagged Cdc25C1 but not Cdc25C5 form during mitosis (Figure S6A), reflecting the presence and absence of the PBD binding site at Thr130, respectively (Elia et al., 2003).

We next investigated when Plk1-dependent Cdc25C1 phosphorylation is taking place. We tracked the temporal regulation of Plk1 interaction with its Cdc25C1 substrate during the cell cycle by immunoprecipitation assays. Interaction between endogenous Plk1 and Cdc25C1 was initiated before entry into mitosis and increased progressively until the mitotic entry peak (~9 hr post-thymidine release), possibly related to Plk1 protein synthesis (Figure 6B). Identification of Plk1-dependent Cdc25C1 phosphorylation sites was addressed by mass spectrometry, following the immunoprecipitation of endogenous Cdc25C1 or a 3xFLAG-YFP-Cdc25C1-tagged form (Figures S6B and S6C). Using complementary protease digestions, ~87% of Cdc25C protein sequence was covered, and 32 phosphorylation sites were identified, 16 of which had been previously reported in phosphoproteomic analyses (Table S1) (Kettenbach et al., 2011). Comparisons of Cdc25C phosphorylation states with or without Plk1 inhibition led to the identification of eight Plk1-dependent phosphosites (Table S1 and Figure S7). Interestingly, all the surrounding sequences fitted with consensus Plk1 phosphorylation sites (Kettenbach et al., 2011). More importantly, Plk1 sites, except for Thr268, were fully conserved in mammals (Ser20, 38, 61, 75) and vertebrates (including *Xenopus laevis*; Ser38, 61, 75) (Figure 6C).

A phospho-specific antibody directed against the fully conserved Ser75 site surrounded by a canonical Plk1 consensus sequence was generated, which recognizes 3xFLAG-tagged Cdc25C1 but not 3xFLAG-Cdc25C1 S75A or 3xFLAG-Cdc25C5 isoform during mitosis (Figure S6D). It showed that S75 phosphorylation during mitosis is dependent on Plk1 activity (Figure S6E). We used this antibody to track Plk1-dependent Cdc25C1 phosphorylation during the cell cycle. A basal Cdc25C1-S75 phosphorylation signal was detectable during S/G2 progression, which significantly increased at the time of mitotic entry and relied on Plk1 activity (Figure 6D). Because the synchronization procedures used are inherently imperfect and provide limited temporal resolution, a FRET-based phosphorylation sensor based on Cdc25C1-S75 phosphosite was generated (Figure S6F). The replacement of Ser75 with a non-phosphorylatable residue and the use of chemical inhibitors

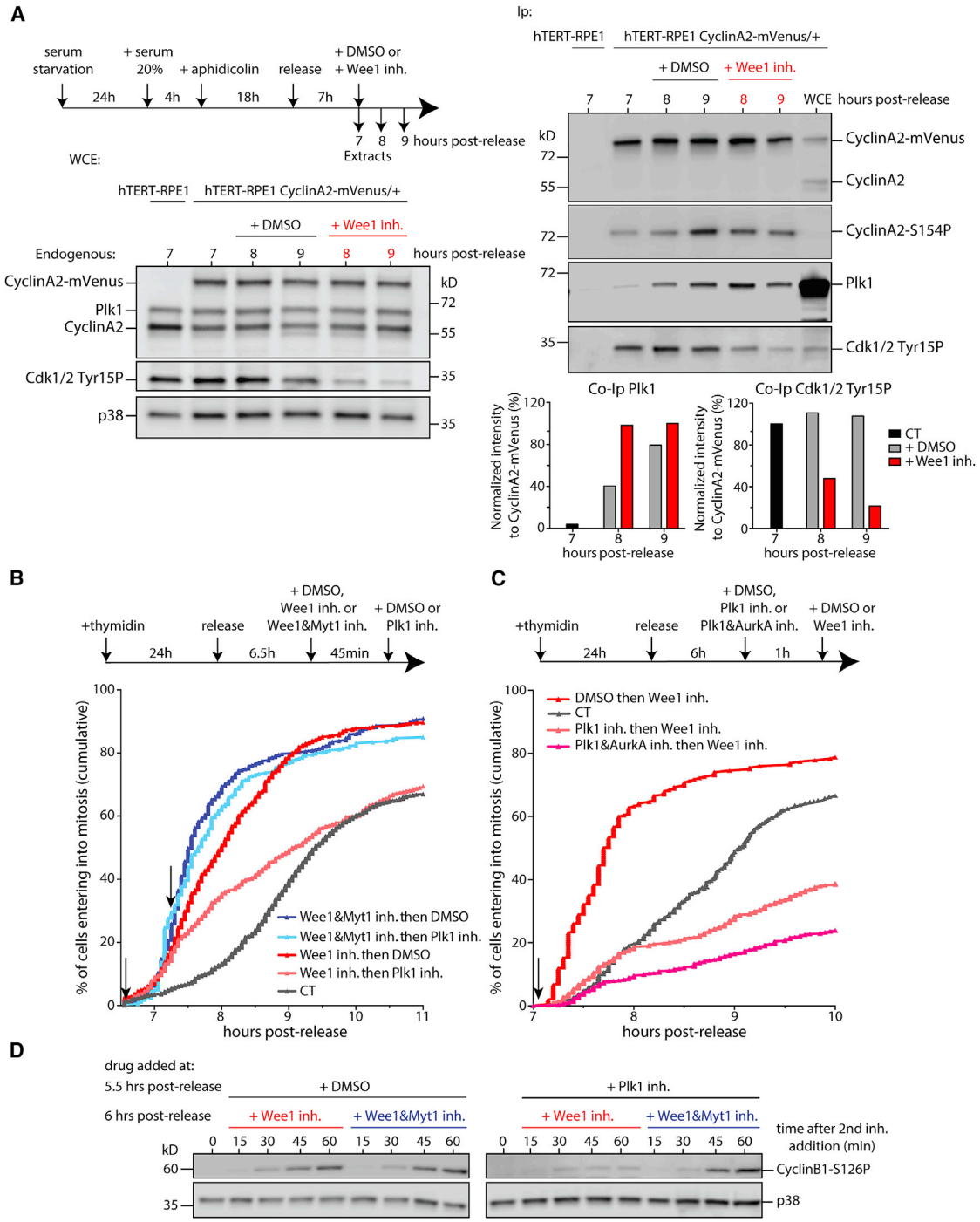

Figure 5. CyclinA2 and Plk1 Progressively Interact during G2

(A) CyclinA2-mVenus/$^{+}$ or normal hTERT-RPE1 cells were synchronized in G2 phase using the indicated procedure (mitotic peak ~10 hr post-release), and immunoprecipitation was performed at reported times using GFP-trap beads. When indicated, Wee1 inhibitor MK-1775 was added at t_{7h} post-release. Immunoblots show the level of various proteins. Left: whole-cell extracts (WCE). Right: immunoprecipitation assays (Ip). Bottom: quantification of Plk1 and Cdk1/2 Tyr15P signals normalized to CyclinA2-mVenus. Data were determined by three independent experiments.

(B and C) Graphs display cumulative mitotic entry over time normalized to cell density (n > 500 cells per condition).

(B) Early G2 synchronized HeLa cells were treated (except in CT, + DMSO) by a Wee1 (MK-1775) or a Wee1&Myt1 (PD0166285) inhibitor. When indicated, Plk1 inhibitor BI2536 was added 45 min later.

(legend continued on next page)

showed that its FRET dynamics is dependent on both Ser75 phosphorylation and Plk1, but not on Mps1, activity (Figures S6F and S6G). Time-lapse recordings showed that the phosphorylation of Cdc25C1-S75 sensor was initiated ~40 min before NEBD, closely mimicking Pk1 activity kinetics previously described (Figure 6E). Hence, it supports that Plk1 promotes Cdc25C1 phosphorylation, at least on Ser75, before mitotic entry. Nonetheless, because Cdc25C1-Ser75 sensor lacks Plk1 PBD binding site, it is possible that the phosphorylation of endogenous Cdc25C1 on Ser75 is initiated earlier during G2 due to the favorable interaction between Plk1 and Cdc25C1.

Previous work reported that Cdc25C phosphatase activity can be stimulated by both Plk1 or CyclinB1-Cdk1 in vitro (Hoffmann et al., 1993; Roshak et al., 2000). We addressed whether Cdc25C1 phosphorylation by Plk1 is sufficient to promote commitment to mitosis. Hence, fluorescent-tagged wild-type (WT)-Cdc25C1 or phospho-mimetic forms of the conserved Plk1 sites in mammals ("5E"; S20-38-61-75-102E; note that site 102 might be missing in C. Lupus) and in vertebrates ("3E"; S38-61-75E) were transiently expressed in HEK293 cells. Following a short synchronization-release regime, cells were trapped into mitosis and analyzed by immunostaining assays (Figure 7A, left). All fluorescent (yellow fluorescent protein; YFP) Cdc25C-tagged forms exhibited an exclusive cytoplasmic localization until NEBD, as previously described (Gavet and Pines, 2010b). The overexpression of WT-Cdc25C1 increased the amount of mitotic cells (CT: 6%; WT-Cdc25C1: 32%), consistent with a previous findings (Bonnet et al., 2008). Whereas the expression of the 3E form did not further increase the number of mitotic cells, the 5E phospho-mimetic form significantly promoted mitosis (3E: 31%; 5E: 48%) (Figure 7A, left). We also performed similar assays in the absence of Plk1 activity (BI2536 200 nM at t_{6h} post-release). Accumulation of YFP positive cells into mitosis was reduced by ~50% under these experimental conditions. Remarkably, cells expressing the 5E form exhibited a different behavior and still significantly entered mitosis (Figure 7A, right). To address more precisely the contribution of Plk1-dependent Cdc25C1 phosphorylation for commitment to mitosis, we performed time-lapse recordings of the different YFP-Cdc25C1-expressing cell populations (Figure 7B). Consistent with our immunofluorescence results, WT-Cdc25C1 and 3E-expressing cells exhibited a similar behavior and entered significantly earlier into mitosis, whereas the 5E phospho-mimetic form further accelerated entry into mitosis by up to 2 hr (based on the time at which 50% of the fluorescent cells have performed mitosis) (Figure 7B, left). Entry into mitosis was also recorded in Plk1 inhibition conditions. Mitotic entry of control cells was massively inhibited, whereas overexpression of WT-Cdc25C1 and 3E form had limited mitosis-promoting effects (Figure 7B, right). Remarkably, the overexpression of the 5E form strongly promoted the transition into mitosis, and all the cells entered mitosis during the time course of the experiment (Figure 7B, right).

Hence, our present findings strongly suggest that the multiple phosphorylation of Cdc25C1 by Plk1 is a key event promoting commitment to mitosis.

DISCUSSION

While a set of regulators of mitotic entry have been previously identified (Lindqvist et al., 2009), a main challenge remains to decipher their relative contribution and how they work in concert to control the transition into mitosis. Here, combining careful evaluation of Plk1 inhibitors in a dose-dependent manner, a chemical genetics model to target Plk1 activity, and time-lapse recordings of asynchronous populations, we demonstrate that entry into mitosis relies on Plk1 activity in mammalian somatic cells. Spindle assembly and/or satisfaction of SAC appear far more sensitive to any interference with Plk1 activity than mitotic entry, and we obtain evidence that a minimal Plk1 activity is sufficient to promote commitment to mitosis. We speculate that it might originate from the anchoring of Plk1 to Cdc25C1 phosphatase, which phosphorylation is sufficient to promote mitotic entry. Hence, the technical limitations to fully inhibit Plk1-dependent Cdc25C1 phosphorylation might provide an explanation for the contradictory results previously reported (Lane and Nigg, 1996; Liu et al., 2006; Seki et al., 2008). Supporting this interpretation, incomplete (up to 90%) versus full Plx1 (Plk1 homolog) depletion in *Xenopus* oocyte extracts delays or fully inhibits CyclinB-Cdk1 activation (Qian et al., 2001). Our current findings are consistent with a recent work reporting a G2 arrest following the use of Plk1 inhibitors, although side effects including potential DNA damages were not ruled out (Aspinall et al., 2015).

We determine that Plk1 activity suddenly rises in late G2 and shortly precedes CyclinB1-Cdk1 activation. Investigating the mechanism by which Plk1 promotes mitotic entry, we identify the Cdc25C1 phosphatase as its major Cdc25 target during G2/M progression. Cdc25C is activated later than Cdc25A and Cdc25B and close to the G2/M transition (Lammer et al., 1998), but its contribution in mitotic entry remained puzzling. Indeed, its partial depletion by RNAi did not affect the kinetics of mitotic entry (our unpublished data), whereas its overexpression had a limited effect that we hypothesize is related to its low phosphatase activity in its unphosphorylated state (Bonnet et al., 2008; Gabrielli et al., 1997; Strausfeld et al., 1994). Plk1 can stimulate Cdc25C phosphatase activity in vitro, but target phosphorylation sites remained unknown (Roshak et al., 2000). Here, we identify several Plk1-dependent Cdc25C1 phosphosites fully conserved in mammals. Endogenous Plk1 and Cdc25C1 progressively interact in interphase, and we provide evidence that Plk1 promotes Cdc25C1 phosphorylation, at least on Ser75, before entry into mitosis. The spatiotemporal regulation of other phosphosites will require further investigations. Supporting the relevance of identified Cdc25C1 phosphosites, overexpression of phosphomimetic mutants promotes entry into mitosis, even in the absence of Plk1 activity. Hence, it supports the notion

(C) Complementary experiments. Early G2 synchronized HeLa cells were treated or not by Aurora-A (MLN8054), Plk1 (BI2536), or both inhibitors at t_{6h} before Wee1 inhibition (MK-1775) 1 hr later (arrow).

(D) Immunoblots showing CyclinB1-S126P phosphorylation profiles over a 1-hr period following Wee1 (MK-1775) or Wee1&Myt1 (PD166285) inhibition on early G2 synchronized HeLa cells (at t_{6h} post-release), preceded or not by the addition of Plk1 inhibitor BI2536 (at $t_{5:30h}$).

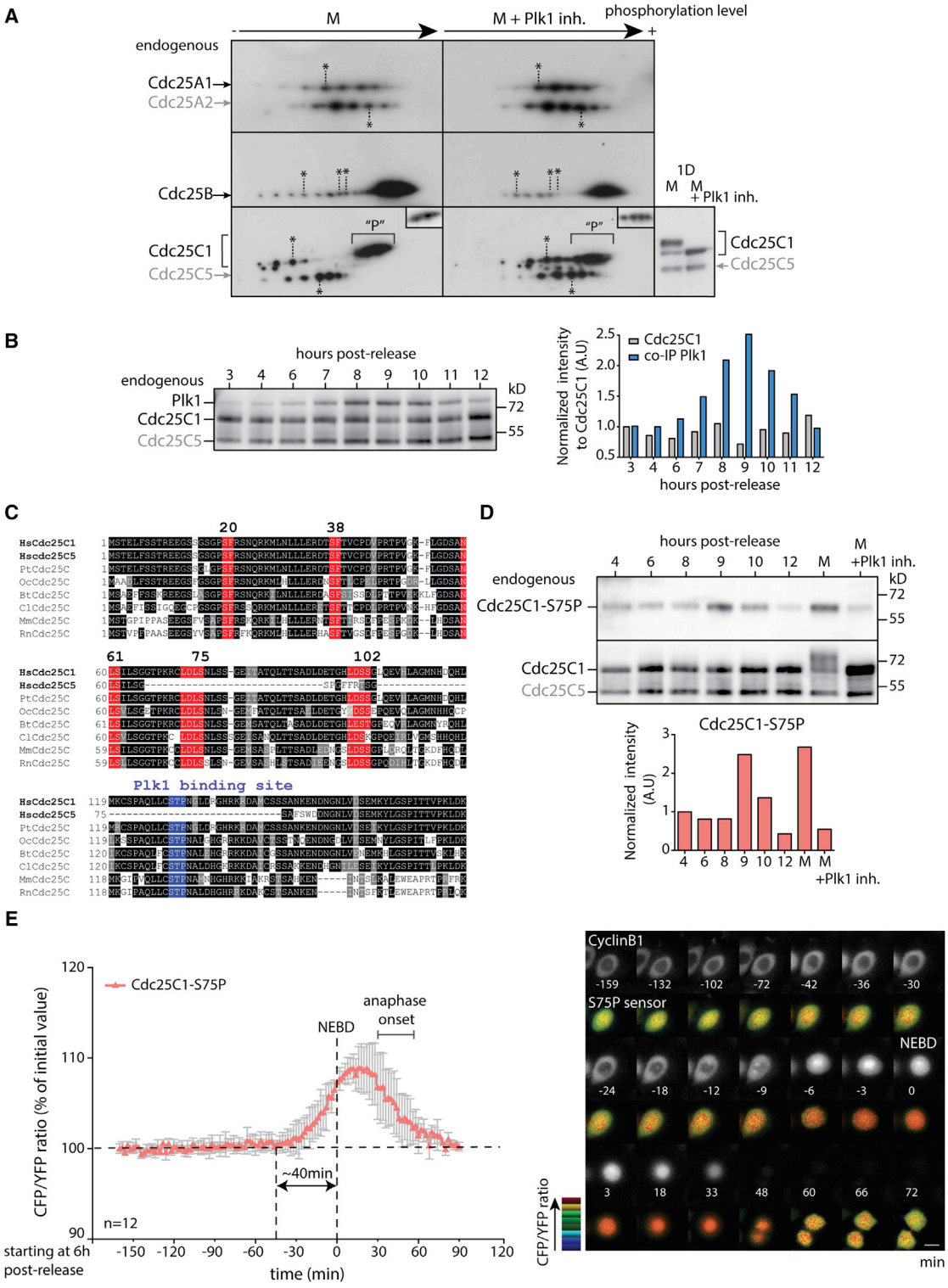

Figure 6. Plk1-Dependent Cdc25C1 Phosphorylation in Late G2

(A) Mitotic arrested HeLa cells (thymidine release + nocodazole) were treated or not with Plk1 inhibitor BI2536 (200 nM) for 1 hr, and samples were analyzed by two-dimensional (2D) immunoblot (1D, right). Note that few minor forms of Cdc25B were close to the detection limit, but highly phosphorylated ones were unaffected by Plk1 inhibition (four independent experiments). For clarity, some identical spots are highlighted using black stars.

(legend continued on next page)

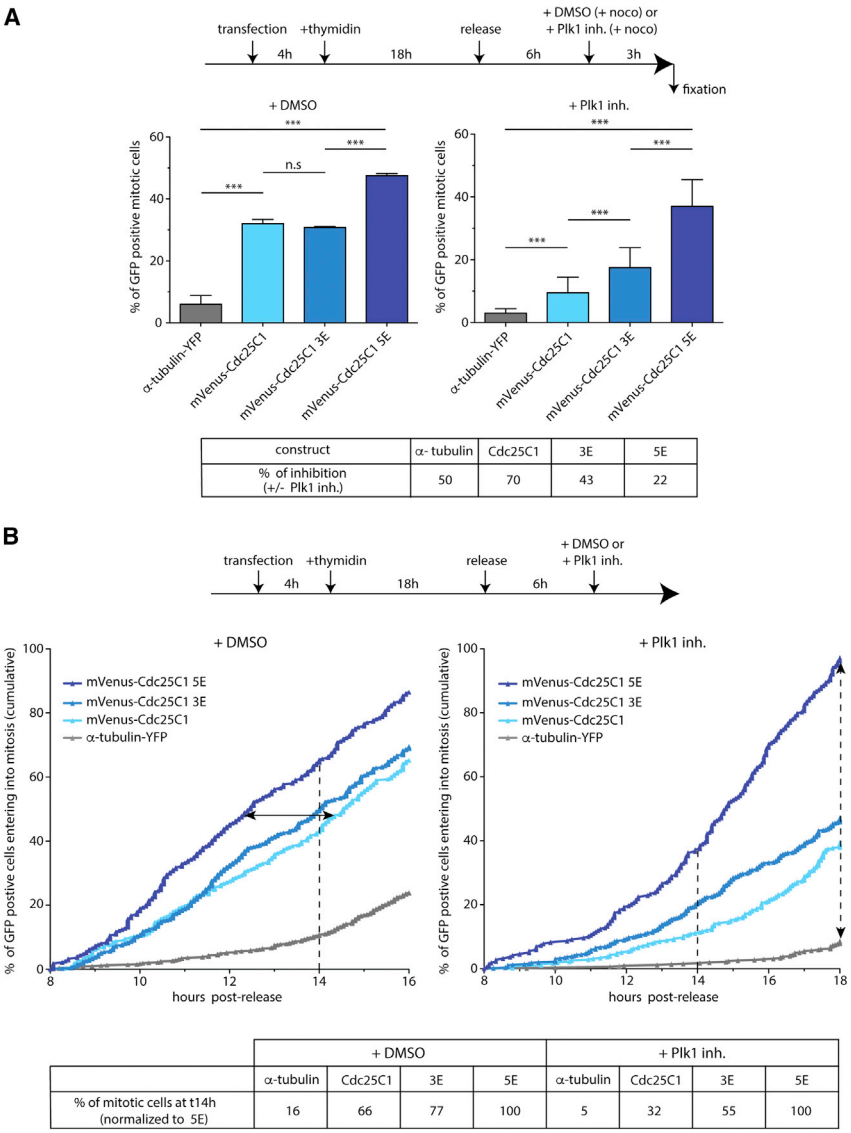

construct	α- tubulin	Cdc25C1	3E	5E
% of inhibition (+/- Plk1 inh.)	50	70	43	22

	+ DMSO				+ Plk1 inh.			
	α-tubulin	Cdc25C1	3E	5E	α-tubulin	Cdc25C1	3E	5E
% of mitotic cells at t14h (normalized to 5E)	16	66	77	100	5	32	55	100

Figure 7. Cdc25C1 Phosphomimetics Forms on Plk1 Sites Promote Entry into Mitosis

(A) Synchronized HEK293 cells expressing either α-tubulin-YFP (CT), mVenus-Cdc25C1, -Cdc25C1-S38,61,75E (3E), or -Cdc25C1-S20,38,61,75,102E (5E) were trapped into mitosis (+ nocodazole at t_{6h} post-thymidine release) and analyzed at t_{9h} post-release using H3S10P and DAPI staining. When indicated, Plk1 inhibitor BI2536 was added at t_{6h}. Data are means ± SD, n = 200 cells analyzed per condition; two independent experiments. Statistical analyses (Fisher's test), ***p value < 0.001. Table: percentages of inhibition of mitotic entry following Plk1 inhibition in indicated conditions.

(B) Left: synchronized HEK293 cells (single thymidine release regime) expressing the indicated constructs (CT: α-tubulin-YFP) were tracked by recording YFP signals at one image/5 min. Mitotic entry was defined as the time of YFP-Cdc25C1 intracellular redistribution at NEBD. Cumulative curves of mitotic entry are shown. Right: Plk1 inhibitor BI2536 was added at t_{6h}. n = 300–500 YFP positive cells were analyzed for each condition. Displayed is a representative experiment from three independent ones performed on either asynchronous or synchronized cells. Table: percentages of cells that have reached mitosis at t_{14h} post-release, following or not Plk1 inhibition.

that Plk1-dependent Cdc25C1 phosphorylation in late G2 is a key event to trigger a timely entry into mitosis. Nonetheless, because Cdc25C or double Cdc25B and C (BCKO) knockout mice are viable, alternative mechanisms must be taking place to trigger mitotic entry (Ferguson et al., 2005). A delay in Cdk1 activation has been reported in the absence of Cdc25B&C (Ferguson et al., 2005). Consistent with our present findings (Figure S2D), it is possible that a persistent accumulation of Plk1 in BCKO cells in which mitosis is delayed might promote Wee1 degradation, ultimately leading to entry into mitosis (Watanabe et al., 2005).

Addition of either CyclinB or CyclinA can promote Plx1 activation in *Xenopus* egg extracts (Abrieu et al., 1998; Lorca et al., 2010). Hence, it remained unclear whether Plk1 activation is initiated by CyclinA2-Cdk or CyclinB1-Cdk1. Our present findings support the former hypothesis providing an outline on how CyclinA2-Cdk contributes to the control of mitotic entry. We observe that Plk1 activation reproducibly precedes CyclinB1-Cdk1 activation and is still taking place following CyclinB1 depletion. We also report that endogenous Plk1 and CyclinA2 interact

(B) Immunoprecipitation of endogenous Cdc25C1&C5 isoforms using anti-Cdc25C antibody at reported times (double thymidine-release regime) from HeLa cell extracts. Immunoblot shows the co-immunoprecipitation of endogenous Plk1. Normalized quantification is also displayed. Data were determined by two independent experiments.

(C) Sequence alignment of NH_2-terminal Cdc25C proteins. Plk1-dependent phosphorylation sites are indicated as well as surrounding consensus sequence (in red). Hs, *Homo sapiens*; Pt, *Pan troglodytes*; Oc, *Oryctolagus cuniculus*; Bt, *Bos Taurus*; Cl, *Canis lupus*; Mm, *Mus musculus*; Rn, *Rattus Norvegicus*.

(D) As in (B), immunoblot showing Cdc25C1-Ser75 phosphorylation level. Note that Ser75 phosphorylation is more prominent on Cdc25C1 lower than higher migrating band, suggesting that they originate from different phosphorylation combinations. Normalized quantification is also displayed. Data were determined by two independent experiments.

(E) Quantification of CFP/YFP emission ratio changes over time of HeLa cells expressing the Cdc25C1-S75P sensor. Curves were aligned on NEBD. Data are means ± SD, n = 12; two independent experiments. Right: IMD representation of CFP/YFP ratio changes and CyclinB1 intracellular localization during time. Bar, 10 μm.

See also Figures S6 and S7 and Table S1.

in a timely regulated manner during G2, related to CyclinA2-Cdk activity rise. Consistently, their interaction is promoted following stimulation of CyclinA2-Cdk activity by Wee1 inhibition. The molecular links between CyclinA2-Cdk and Plk1 remain to be investigated to distinguish between several, not mutually exclusive, scenarios. First, CyclinA2-Cdk could induce Aurora-A activation during G2 because Aurora-A-dependent Plk1 Thr210 phosphorylation is rapidly promoted following CyclinA2-Cdk stimulation. Second, CyclinA2-Cdk1/2 might phosphorylate hBora and promote Aurora-A-dependent Plk1 activation (Tavernier et al., 2015). Third, direct Cdk-dependent T-loop phosphorylation might be required for Plk1 activity, as observed for Cdc5 *S. cerevisiae* homolog (Dulla et al., 2010; Mortensen et al., 2005). Alternatively, Plk1 activation may be initiated by Aurora-A/Bora and further boosted before mitotic entry by CyclinA2-Cdk-dependent Bora and/or Plk1 phosphorylation (Lasek et al., 2016; Thomas et al., 2016).

Future work on the mechanisms leading to the activation of Plk1 by CyclinA2-Cdk, an S-promoting factor, should help to unravel how the coordination between DNA replication and mitotic entry is reproducibly achieved during the cell cycle.

EXPERIMENTAL PROCEDURES

Detailed experimental procedures, reagents, and antibodies used are described in the Supplemental Experimental Procedures.

Cell Culture

Human cervix adenocarcinoma (HeLa) and embryonic kidney (HEK293) cells were cultured in DMEM, high glucose (Life Technologies), supplemented with 10% fetal calf serum (FCS), 2 mM glutamine, 100 U/mL penicillin, and 100 μg/mL streptomycin. HeLa PCNA-RFP stable cell line is a kind gift from J. Pines's laboratory. WT- (ATCC CRL-4000), mRuby-PCNA/$^{+}$ knockin, CyclinA2-mVenus/$^{+}$ mRuby-PCNA/$^{+}$ double knockin, *PLK1*$^{\Delta/\Delta}$-EGFP-Plk1^{wt} and *PLK1*$^{\Delta/\Delta}$-EGFP-Plk1^{as} (Burkard et al., 2007), and hTERT-RPE1 cells were maintained in DMEM/F12 (Life Technologies) supplemented with 10% FCS, 100 U/mL penicillin, and 100 μg/mL streptomycin.

HeLa and HEK293 cells were synchronized by a single (video-microscopy assays) or a double (immunoblots) thymidine-release regime (2.5 mM for 18 or 24 hr or following a 18/10/18-hr schedule, respectively). hTERT-RPE1 cells were synchronized by a serum starvation-release regime (FCS 0.1% for 24 hr) (mitotic peak at ~26 hr post-release) or using serum starvation conditions followed by an aphidicolin treatment (1 μM) for 18 hr for immunoprecipitation assays (mitotic peak at ~10 hr post-release). Nocodazole was used to trap cells into mitosis.

Time-Lapse Imaging

For phase-contrast time-lapse imaging assays, cells were seeded in 12-well tissue culture plates and imaged in CO_2-independent L15 medium without phenol red (Life Technologies) supplemented with 10% FCS, at 20× using an inverted video-microscope (Olympus IX83) equipped with an ORCA flash 4.0 camera and controlled by CellSens software.

For FRET imaging assays, HeLa cells were seeded on glass-bottom dishes (μ-Dish, IBIDI), precoated with fibronectin (Sigma-Aldrich) at 1 μg/cm^2 and imaged in L15 without phenol red supplemented with 1% FCS. Imaging was performed using an inverted microscope (Leica DMI6000) controlled by Metamorph software and equipped with adaptive focus control, fast emission filter wheel (lambda 10-3, Sutter), electron multiplying charge coupled device (EMCCD) camera (Evolve 512; Photometrics), HCX PL APO 40×/NA 1.30 oil immersion lens, and light-emitting diode (LED)-based illumination system (spectra X-light engine, Lumencor). Filters used were ET480/40m and ET535/30m and double band CFP/YFP dichroic mirror 51017bs from Chroma (Chroma Technology). Quantifications were performed using ImageJ software (Gavet and Pines, 2010a). Intensity-modulated display (IMD) representations were performed using Metamorph software.

Plasmid Constructs

Complete sequences are available upon request.

SUPPLEMENTAL INFORMATION

Supplemental Information includes Supplemental Experimental Procedures, seven figures, and one table and can be found with this article online at http://dx.doi.org/10.1016/j.celrep.2017.05.031.

AUTHOR CONTRIBUTIONS

Conceptualization, O.G. and L.G.; Methodology, L.G. and J.M.; Investigation, O.G., L.G., D.L., and B.L.; Writing – Original Draft, O.G. and L.G.; Writing – Review & Editing, O.G.; Funding Acquisition, O.G.; Supervision, O.G.

ACKNOWLEDGMENTS

We thank Dr. Lionel Pintard for critical reading of the manuscript. We are very grateful to Dr. Prasad Jallepalli and Dr. Jonathon Pines for providing us HeLa and hTERT-RPE1 cell lines and Dr. Mounira Amor-Gueret for hosting L.G. and O.G. in her laboratory. This project was funded by the Ligue Nationale contre le Cancer (6FI10696MLCH), Fondation ARC pour la recherche sur le cancer (SFI20111203951), Cancéropôle-Ile de France (2012-2-INV-05-IC-1), and Agence Nationale de la Recherche (13-BSV2-0016-01). J.M. is supported by the German Research Foundation (DFG) (Emmy Noether; MA 5831/1-1) and receives funding from the European Research Council (ERC) under the European Union's Horizon 2020 research and innovation program (grant agreement no. 680042).

Received: December 2, 2016
Revised: April 8, 2017
Accepted: May 9, 2017
Published: June 6, 2017

REFERENCES

Abrieu, A., Brassac, T., Galas, S., Fisher, D., Labbé, J.C., and Dorée, M. (1998). The Polo-like kinase Plx1 is a component of the MPF amplification loop at the G2/M-phase transition of the cell cycle in Xenopus eggs. J. Cell Sci. *111*, 1751–1757.

Akopyan, K., Silva Cascales, H., Hukasova, E., Saurin, A.T., Müllers, E., Jaiswal, H., Hollman, D.A., Kops, G.J., Medema, R.H., and Lindqvist, A. (2014). Assessing kinetics from fixed cells reveals activation of the mitotic entry network at the S/G2 transition. Mol. Cell *53*, 843–853.

Albert, H., Santos, S., Battaglia, E., Brito, M., Monteiro, C., and Bagrel, D. (2011). Differential expression of CDC25 phosphatases splice variants in human breast cancer cells. Clin. Chem. Lab Med *49*, 1707–1714.

Aspinall, C.F., Zheleva, D., Tighe, A., and Taylor, S.S. (2015). Mitotic entry: Non-genetic heterogeneity exposes the requirement for Plk1. Oncotarget *6*, 36472–36488.

Bonnet, J., Coopman, P., and Morris, M.C. (2008). Characterization of centrosomal localization and dynamics of Cdc25C phosphatase in mitosis. Cell Cycle *7*, 1991–1998.

Booher, R.N., Holman, P.S., Fattaey, A., and Fattaey, A. (1997). Human Myt1 is a cell cycle-regulated kinase that inhibits Cdc2 but not Cdk2 activity. J. Biol. Chem. *272*, 22300–22306.

Bruinsma, W., Macurek, L., Freire, R., Lindqvist, A., and Medema, R.H. (2014). Bora and Aurora-A continue to activate Plk1 in mitosis. J. Cell Sci. *127*, 801–811.

Burkard, M.E., Santamaria, A., and Jallepalli, P.V. (2012). Enabling and disabling polo-like kinase 1 inhibition through chemical genetics. ACS Chem. Biol. *7*, 978–981.

Burkard, M.E., Randall, C.L., Larochelle, S., Zhang, C., Shokat, K.M., Fisher, R.P., and Jallepalli, P.V. (2007). Chemical genetics reveals the requirement for Polo-like kinase 1 activity in positioning RhoA and triggering cytokinesis in human cells. Proc. Natl. Acad. Sci. USA *104*, 4383–4388.

Coulonval, K., Bockstaele, L., Paternot, S., and Roger, P.P. (2003). Phosphorylations of cyclin-dependent kinase 2 revisited using two-dimensional gel electrophoresis. J. Biol. Chem. *278*, 52052–52060.

Dulla, K., Daub, H., Hornberger, R., Nigg, E.A., and Körner, R. (2010). Quantitative site-specific phosphorylation dynamics of human protein kinases during mitotic progression. Mol. Cell Proteomics *9*, 1167–1181.

Elia, A.E., Rellos, P., Haire, L.F., Chao, J.W., Ivins, F.J., Hoepker, K., Mohammad, D., Cantley, L.C., Smerdon, S.J., and Yaffe, M.B. (2003). The molecular basis for phosphodependent substrate targeting and regulation of Plks by the Polo-box domain. Cell *115*, 83–95.

Ferguson, A.M., White, L.S., Donovan, P.J., and Piwnica-Worms, H. (2005). Normal cell cycle and checkpoint responses in mice and cells lacking Cdc25B and Cdc25C protein phosphatases. Mol. Cell. Biol. *25*, 2853–2860.

Fung, T.K., Ma, H.T., and Poon, R.Y.C. (2007). Specialized roles of the two mitotic cyclins in somatic cells: Cyclin A as an activator of M phase-promoting factor. Mol. Biol. Cell *18*, 1861–1873.

Furuno, N., den Elzen, N., Pines, J., Den Elzen, N., Pines, J., den Elzen, N., Pines, J., Den Elzen, N., and Pines, J. (1999). Human cyclin A is required for mitosis until mid prophase. J. Cell Biol. *147*, 295–306.

Gabrielli, B.G., Clark, J.M., McCormack, A.K., and Ellem, K.A.O. (1997). Hyperphosphorylation of the N-terminal domain of Cdc25 regulates activity toward cyclin B1/Cdc2 but not cyclin A/Cdk2. J. Biol. Chem. *272*, 28607–28614.

Gaffré, M., Martoriati, A., Belhachemi, N., Chambon, J.P., Houliston, E., Jessus, C., and Karaiskou, A. (2011). A critical balance between cyclin B synthesis and Myt1 activity controls meiosis entry in Xenopus oocytes. Development *138*, 3735–3744.

Gavet, O., and Pines, J. (2010a). Progressive activation of CyclinB1-Cdk1 coordinates entry to mitosis. Dev. Cell *18*, 533–543.

Gavet, O., and Pines, J. (2010b). Activation of cyclin B1-Cdk1 synchronizes events in the nucleus and the cytoplasm at mitosis. J. Cell Biol. *189*, 247–259.

Gilmartin, A.G., Bleam, M.R., Richter, M.C., Erskine, S.G., Kruger, R.G., Madden, L., Hassler, D.F., Smith, G.K., Gontarek, R.R., Courtney, M.P., et al. (2009). Distinct concentration-dependent effects of the polo-like kinase 1-specific inhibitor GSK461364A, including differential effect on apoptosis. Cancer Res. *69*, 6969–6977.

Goldstone, S., Pavey, S., Forrest, A., Sinnamon, J., and Gabrielli, B. (2001). Cdc25-dependent activation of cyclin A/cdk2 is blocked in G2 phase arrested cells independently of ATM/ATR. Oncogene *20*, 921–932.

Gong, D., Pomerening, J.R., Myers, J.W., Gustavsson, C., Jones, J.T., Hahn, A.T., Meyer, T., and Ferrell, J.E., Jr. (2007). Cyclin A2 regulates nuclear-envelope breakdown and the nuclear accumulation of cyclin B1. Curr. Biol. *17*, 85–91.

Hoffmann, I., Clarke, P.R., Marcote, M.J., Karsenti, E., and Draetta, G. (1993). Phosphorylation and activation of human cdc25-C by cdc2–cyclin B and its involvement in the self-amplification of MPF at mitosis. EMBO J. *12*, 53–63.

Jackman, M., Lindon, C., Nigg, E.A., and Pines, J. (2003). Active cyclin B1-Cdk1 first appears on centrosomes in prophase. Nat. Cell Biol. *5*, 143–148.

Karlsson, C., Katich, S., Hagting, A., Hoffmann, I., and Pines, J. (1999). Cdc25B and Cdc25C differ markedly in their properties as initiators of mitosis. J. Cell Biol. *146*, 573–584.

Kettenbach, A.N., Schweppe, D.K., Faherty, B.K., Pechenick, D., Pletnev, A.A., and Gerber, S.A. (2011). Quantitative phophoproteomics identifies substrates and functional modules of Aurora and Polo-like kinase activities in mitotic cells. Sci. Signal. *4*, rs5.

Lammer, C., Wagerer, S., Saffrich, R., Mertens, D., Ansorge, W., and Hoffmann, I. (1998). The cdc25B phosphatase is essential for the G2/M phase transition in human cells. J. Cell Sci. *111*, 2445–2453.

Lane, H.A., and Nigg, E.A. (1996). Antibody microinjection reveals an essential role for human polo-like kinase 1 (Plk1) in the functional maturation of mitotic centrosomes. J. Cell Biol. *135*, 1701–1713.

Lasek, A.L., McPherson, B.M., Trueman, N.G., and Burkard, M.E. (2016). The Functional Significance of Posttranslational Modifications on Polo-Like Kinase 1 Revealed by Chemical Genetic Complementation. PLoS ONE *11*, e0150225.

Lee, G., White, L.S., Hurov, K.E., Stappenbeck, T.S., and Piwnica-Worms, H. (2009). Response of small intestinal epithelial cells to acute disruption of cell division through CDC25 deletion. Proc. Natl. Acad. Sci. USA *106*, 4701–4706.

Lindqvist, A., Rodríguez-Bravo, V., Medema, R.H., and Rodríguez-Bravo, V. (2009). The decision to enter mitosis: Feedback and redundancy in the mitotic entry network. J. Cell Biol. *185*, 193–202.

Liu, X., Lei, M., and Erikson, R.L. (2006). Normal cells, but not cancer cells, survive severe Plk1 depletion. Mol. Cell. Biol. *26*, 2093–2108.

Liu, D., Davydenko, O., and Lampson, M.A. (2012). Polo-like kinase-1 regulates kinetochore-microtubule dynamics and spindle checkpoint silencing. J. Cell Biol. *198*, 491–499.

Lobjois, V., Froment, C., Braud, E., Grimal, F., Burlet-Schiltz, O., Ducommun, B., and Bouche, J.-P. (2011). Study of the docking-dependent PLK1 phosphorylation of the CDC25B phosphatase. Biochem. Biophys. Res. Commun. *410*, 87–90.

Lorca, T., Bernis, C., Vigneron, S., Burgess, A., Brioudes, E., Labbé, J.C., and Castro, A. (2010). Constant regulation of both the MPF amplification loop and the Greatwall-PP2A pathway is required for metaphase II arrest and correct entry into the first embryonic cell cycle. J. Cell Sci. *123*, 2281–2291.

Lu, L.-Y., Wood, J.L., Minter-Dykhouse, K., Ye, L., Saunders, T.L., Yu, X., and Chen, J. (2008). Polo-like kinase 1 is essential for early embryonic development and tumor suppression. Mol. Cell. Biol. *28*, 6870–6876.

Macůrek, L., Lindqvist, A., Lim, D., Lampson, M.A., Klompmaker, R., Freire, R., Clouin, C., Taylor, S.S., Yaffe, M.B., and Medema, R.H. (2008). Polo-like kinase-1 is activated by aurora A to promote checkpoint recovery. Nature *455*, 119–123.

Marumoto, T., Hirota, T., Morisaki, T., Kunitoku, N., Zhang, D., Ichikawa, Y., Sasayama, T., Kuninaka, S., Mimori, T., Tamaki, N., et al. (2002). Roles of aurora-A kinase in mitotic entry and G2 checkpoint in mammalian cells. Genes Cells *7*, 1173–1182.

McKinley, K.L., and Cheeseman, I.M. (2014). Polo-like kinase 1 licenses CENP-A deposition at centromeres. Cell *158*, 397–411.

Mortensen, E.M., Haas, W., Gygi, M., Gygi, S.P., and Kellogg, D.R. (2005). Cdc28-dependent regulation of the Cdc5/Polo kinase. Curr. Biol. *15*, 2033–2037.

Nakajima, H., Toyoshima-Morimoto, F., Taniguchi, E., and Nishida, E. (2003). Identification of a consensus motif for Plk (Polo-like kinase) phosphorylation reveals Myt1 as a Plk1 substrate. J. Biol. Chem. *278*, 25277–25280.

Pagano, M., Pepperkok, R., Verde, F., Ansorge, W., and Draetta, G. (1992). Cyclin A is required at two points in the human cell cycle. EMBO J. *11*, 961–971.

Pagliuca, F.W., Collins, M.O., Lichawska, A., Zegerman, P., Choudhary, J.S., and Pines, J. (2011). Quantitative proteomics reveals the basis for the biochemical specificity of the cell-cycle machinery. Mol. Cell. *43*, 406–417.

Qian, Y.W., Erikson, E., Taieb, F.E., and Maller, J.L. (2001). The polo-like kinase Plx1 is required for activation of the phosphatase Cdc25C and cyclin B-Cdc2 in Xenopus oocytes. Mol. Biol. Cell *12*, 1791–1799.

Roshak, A.K., Capper, E.A., Imburgia, C., Fornwald, J., Scott, G., and Marshall, L.A. (2000). The human polo-like kinase, PLK, regulates cdc2/cyclin B through phosphorylation and activation of the cdc25C phosphatase. Cell. Signal. *12*, 405–411.

Seki, A., Coppinger, J.A., Jang, C.-Y., Yates, J.R., and Fang, G. (2008). Bora and the kinase Aurora a cooperatively activate the kinase Plk1 and control mitotic entry. Science *320*, 1655–1658.

Steegmaier, M., Hoffmann, M., Baum, A., Lénárt, P., Petronczki, M., Krssák, M., Gürtler, U., Garin-Chesa, P., Lieb, S., Quant, J., et al. (2007). BI 2536, a potent and selective inhibitor of polo-like kinase 1, inhibits tumor growth in vivo. Curr. Biol. *17*, 316–322.

Strausfeld, U., Fernandez, A., Capony, J.P., Girard, F., Lautredou, N., Derancourt, J., Labbe, J.C., and Lamb, N.J. (1994). Activation of p34cdc2 protein kinase by microinjection of human cdc25C into mammalian cells. Requirement for prior phosphorylation of cdc25C by p34cdc2 on sites phosphorylated at mitosis. J. Biol. Chem. *269*, 5989–6000.

Sumara, I., Giménez-Abián, J.F., Gerlich, D., Hirota, T., Kraft, C., de la Torre, C., Ellenberg, J., and Peters, J.M. (2004). Roles of polo-like kinase 1 in the assembly of functional mitotic spindles. Curr. Biol. *14*, 1712–1722.

Tavernier, N., Noatynska, A., Panbianco, C., Martino, L., Van Hove, L., Schwager, F., Léger, T., Gotta, M., and Pintard, L. (2015). Cdk1 phosphorylates SPAT-1/Bora to trigger PLK-1 activation and drive mitotic entry in C. elegans embryos. J. Cell Biol. *208*, 661–669.

Thomas, Y., Cirillo, L., Panbianco, C., Martino, L., Tavernier, N., Schwager, F., Van Hove, L., Joly, N., Santamaria, A., Pintard, L., and Gotta, M. (2016). Cdk1 phosphorylates SPAT-1/Bora to promote Plk1 activation in C. elegans and human cells. Cell Rep. *15*, 510–518.

Van Horn, R.D., Chu, S., Fan, L., Yin, T., Du, J., Beckmann, R., Mader, M., Zhu, G., Toth, J., Blanchard, K., and Ye, X.S. (2010). Cdk1 activity is required for mitotic activation of aurora A during G2/M transition of human cells. J. Biol. Chem. *285*, 21849–21857.

van Vugt, M.A.T.M., Brás, A., Medema, R.H., and Bras, A. (2004). Polo-like kinase-1 controls recovery from a G2 DNA damage-induced arrest in mammalian cells. Mol. Cell *15*, 799–811.

Violin, J.D., Zhang, J., Tsien, R.Y., and Newton, A.C. (2003). A genetically encoded fluorescent reporter reveals oscillatory phosphorylation by protein kinase C. J. Cell Biol. *161*, 899–909.

Wachowicz, P., Fernández-Miranda, G., Marugán, C., Escobar, B., and de Cárcer, G. (2016). Genetic depletion of Polo-like kinase 1 leads to embryonic lethality due to mitotic aberrancies. BioEssays *38* (*Suppl 1*), S96–S106.

Watanabe, N., Arai, H., Iwasaki, J., Shiina, M., Ogata, K., Hunter, T., and Osada, H. (2005). Cyclin-dependent kinase (CDK) phosphorylation destabilizes somatic Wee1 via multiple pathways. Proc. Natl. Acad. Sci. USA *102*, 11663–11668.

Zabludoff, S.D., Deng, C., Grondine, M.R., Sheehy, A.M., Ashwell, S., Caleb, B.L., Green, S., Haye, H.R., Horn, C.L., Janetka, J.W., et al. (2008). AZD7762, a novel checkpoint kinase inhibitor, drives checkpoint abrogation and potentiates DNA-targeted therapies. Mol. Cancer Ther *7*, 2955–2966.